Case Studies in Thermal Engineering 28 (2021) 101602

Contents lists available at ScienceDirect

Case Studies in Thermal Engineering

journal homepage: www.elsevier.com/locate/csite

The nanofluid flows in the channel with linearly varying wall temperature

Kai-Xin Hu [a,*], Yan Huang [a], Xin-Yuan Zhang [a], Sheng Wang [a], Qi-Sheng Chen [b,c]

[a] Key Laboratory of Impact and Safety Engineering, Ministry of Education, School of Mechanical Engineering and Mechanics, Ningbo University, Ningbo, Zhejiang 315211, China
[b] School of Engineering Science, University of Chinese Academy of Sciences, Beijing 100190, China
[c] Key Laboratory of Microgravity, Institute of Mechanics, Chinese Academy of Sciences, Beijing 100190, China

ARTICLE INFO

Keywords:
Nanofluids
Poiseuille flow
Heat transfer
Nanoparticle concentration
Viscosity stratification

ABSTRACT

In many applications of heat exchanger, due to the heat convection, the wall temperature of the channel usually varies along the streamwise direction. The present paper reports the analysis of nanofluid flows in the channel with linearly varying wall temperature. The non-uniform equilibrium fluid medium model proposed by Buongiorno is applied, where the Brownian diffusion and thermophoresis of nanoparticles are considered. The numerical solutions of laminar flows are determined by the iteration method in conjunction with the Chebyshev collocation method. The results show that: (1) there is a Gaussian distribution of nanoparticle concentration in the wall-normal direction for convective cooling, while its standard deviation depends on the Peclet number and the ratio of Brownian diffusivity to thermophoretic diffusivity; (2) there are obvious stratifications for the viscosity and thermal conductivity in the flow; (3) the velocity decreases significantly with the increase of nanoparticle concentration for convective heating, while there is only a little decrease for the velocity in the cold region for convective cooling.

1. Introduction

Nanofluids, introduced by Choi in 1995 [1], are the colloidal suspensions obtained from dispersing nanoparticles in base fluids. In these fluids, nanometre-sized (<100 nm) particles such as metal, oxide, carbide or carbon nanotubes are suspended in the base fluids such as water and ethylene glycol [2]. In the past two decades, nanofluids have received much attention for their remarkably improved thermal properties [3] and great application potentials in aerospace, energy, electronics, chemical industry et al. [4].

Many works on nanofluids have been devoted to the study of their thermophysical properties (e.g., thermal conductivity, heat transfer coefficients, viscosity, density) [5], preparation methods [6] and transport characteristics in porous media [7]. Some rheological experiments have shown that nanofluids have non-Newtonian behavior [8]. Recently, the properties of nanofluids flows have been investigated by many authors by analytical and numerical methods [9–12]. Simple mathematical models are adopted to describe the mechanical properties of nanofluids from a macroscopic perspective based on the continuous-medium approximation. The numerical studies of convective heat transfer of nanofluids have been reviewed by Vanaki, Ganesan & Mohammed [13].

Two main models are widely used in these theoretical studies for nanofluid flows. The first is the homogeneous fluid medium model proposed by Choi [1]. Si et al. [14]have used this single-phase model to study the mixed convection flow and heat transfer of

* Corresponding author.
E-mail address: hukaixin@nbu.edu.cn (K.-X. Hu).

https://doi.org/10.1016/j.csite.2021.101602
Received 23 June 2021; Received in revised form 13 August 2021; Accepted 26 October 2021
Available online 27 October 2021

pseudo-plastic power law nanofluids past a stretching vertical plate. Dual solutions have been obtained for some values of the physical parameters. However, this model ignores the non-uniformity of the distribution of nanoparticles, which is also significantly different from the experimental results [15]. The second is the non-uniform equilibrium fluid medium model proposed by Buongiorno [15], where the nanoparticle concentration is determined by considering the Brownian diffusion and thermophoresis. Garoosi & Talebi [16] have studied the conjugate natural and mixed convection heat transfer of nanofluids in a square cavity by Buongiorno model. The results suggest that there are lower and higher nanoparticles concentration around the heat sources and sinks, respectively. Therefore, the non-uniform model can describe the flow properties of nanofluids more accurately.

In many applications of heat exchanger, due to the heat convection, the wall temperature of the channel usually varies along the streamwise direction. For this reason, some authors have turned to the problems of channel flows with non-uniform wall temperature. Ostrach [17] has examined the combined natural and forced convection laminar flow and heat transfer of fluids in channels with linearly varying wall temperatures. It was found that the velocities and temperatures decrease with increasing values of the modified Rayleigh number. The laminar flow forced convection in ducts with several boundary conditions have been reviewed by Shah & London [18], including the case with non-uniform wall temperature. However so far, to our best knowledge, no studies have been carried out for the nanofluid flows in channels with varying wall temperatures. It is highly desirable to solve this problem for its great practical importance, which is the purpose of this paper.

In the present work, the plane Poiseuille flow of nanofluids in a channel with linearly varying wall temperature is investigated numerically. The non-homogeneous equilibrium model is used to describe the coupling of nanoparticle motion, fluid flows and heat transfer. Two viscosity models of nanofluids are considered, which are the theoretical model given by Brickman [19] and the empirical model of water–γAl_2O_3 presented by Maiga et al. [20].The solutions of laminar flows are derived, and the stratifications of nanoparticles, viscosity and thermal conductivity are demonstrated.

The paper is organized as follows. In Section 2, the physical model and mathematical formulation of the problem are presented, while the dimensionless governing equations are derived and the numerical methods are illustrated. Then in Section 3, the distributions of velocity, temperature, particle volume fraction, thermal conductivity and viscosity at different parameters are displayed, the effect of temperature on the viscosity is discussed, and comparisons are made with different viscosity models. Finally, our conclusions are drawn in Section 4.

2. Problem formulation

Here, we consider the plane Poiseuille flow in Fig. 1, where a steady flow between two fixed parallel planes is driven by a constant pressure gradient. x and y are the streamwise and wall-normal direction, respectively. p is the pressure. The channel has linearly varying wall temperatureT_b. We assume that the temperature in the flow region T is linear in x plus a distribution in y, and the temperature variation in the normal direction is much larger than that in the streamwise direction. So the variations of viscosity and velocity in x direction are neglected. The flow is parallel and u is the velocity, which only depends on y.

Generally, there are two models which are suitable for simulation of the nanofluids: Manninen's two phase model and Buongiorno's model. The first model is suitable when the size of the nanoparticles is larger than the 100 nm [21]. However, in this paper, we only considered the alumina nanoparticles in the tens of nanometers. Therefore, we use the Buongiorno's model in the following.

2.1. Governing equations

We use the non-uniform equilibrium model to describe the nanofluid flow. The continuity equation is

$$\nabla \cdot \mathbf{u} = 0, \tag{2.1}$$

which is satisfied as the flow is parallel. The momentum equation with negligible external forces is

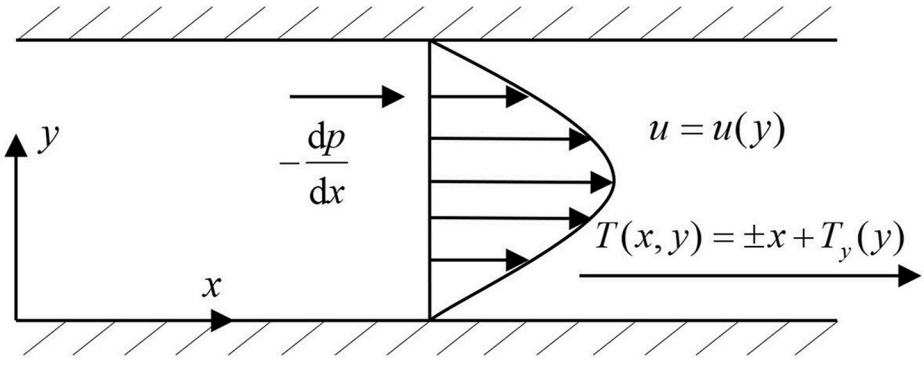

Fig. 1. The plane Poiseuille flow of nanofluids in the channel with linearly varying wall temperature.

$$\rho\left(\frac{\partial \mathbf{u}}{\partial t}+\mathbf{u}\cdot\nabla\mathbf{u}\right)=-\nabla p+\nabla\cdot\boldsymbol{\tau}, \tag{2.2}$$

where $\boldsymbol{\tau}$ is the stress tensor and $\rho$is the density. They can be expressed as follows:

$$\boldsymbol{\tau}=\mu\left(\nabla\mathbf{u}+(\nabla\mathbf{u})^{\mathrm{T}}\right), \tag{2.3}$$

$$\rho=\varphi\rho_s+(1-\varphi)\rho_f, \tag{2.4}$$

where $\mu$is the viscosity, $\varphi$is the nanoparticle concentration (particle volume fraction), $\rho_s,\rho_f,\rho$are the densities of the nanoparticle, the base fluid and the nanofluid.

For the heat transfer in the nanofluid, we consider the convection, conduction and the nanoparticle diffusion. So the energy equation is:

$$\rho c\left(\frac{\partial T}{\partial t}+\mathbf{u}\cdot\nabla T\right)=\nabla\cdot(k\nabla T)+(\rho c)_s\left(D_B\nabla\varphi+D_T\frac{\nabla T}{T}\right)\cdot\nabla T, \tag{2.5}$$

where c is the specific heat of the nanofluid, k is the nanofluid thermal conductivity. It goes

$$\rho c=\varphi(\rho c)_s+(1-\varphi)(\rho c)_f, \tag{2.6}$$

where the subscripts s & f stand for nanoparticle and base fluid, respectively. Usually$(\rho c)_s,(\rho c)_f$ have the same order, for example,$(\rho c)_s\sim 3.1\times10^6\mathrm{J}/(\mathrm{m}^3\cdot\mathrm{K})$ for alumina while $(\rho c)_f\sim 4.2\times10^6\mathrm{J}/(\mathrm{m}^3\cdot\mathrm{K})$ for water [15]. Meanwhile, φ is small, so the variation of ρc in the y direction is neglected in this paper. D_B is the Brownian diffusion coefficient, D_T is the thermal diffusion coefficient,

$$D_B=\frac{k_BT}{3\pi\mu d_s},\quad D_T=\beta\frac{\mu_f}{\rho_f}\varphi. \tag{2.7}$$

Here, k_B is Boltzmann constant, d_s is the diameter of the nanoparticle,

$$\beta=0.26\frac{k_f}{2k_f+k_s}, \tag{2.8}$$

k_s,k_f are the thermal conductivities for nanoparticle and base fluid, respectively.μ_f is the viscosity of the base fluid.

The governing equation of nanoparticles without chemical reactions is:

$$\frac{\partial\varphi}{\partial t}+\mathbf{u}\cdot\nabla\varphi=\nabla\cdot\left(D_B\nabla\varphi+D_T\frac{\nabla T}{T}\right). \tag{2.9}$$

In the fluid, the viscosity and thermal conductivity depend on the particle concentration. We use two simple models to predict the viscosity. The first is presented by Brickman [19]:

$$\mu=\mu_f/(1-\varphi)^{2.5}. \tag{2.10}$$

The other is presented by Maiga et al. [20] for water–γAl_2O_3:

$$\mu=\mu_f\left(1+7.3\varphi+123\varphi^2\right). \tag{2.11}$$

These two models are independent of the temperature. However, when the temperature difference in y direction is big enough, we should consider the effect of temperature on the viscosity. In this work, the temperature dependent viscosity model is as follows [22]:

$$\mu_{fT}=\mu_0\exp\left(\varsigma+\xi\left(\frac{T_0}{T}\right)+\zeta\left(\frac{T_0}{T}\right)^2\right), \tag{2.12}$$

$$\mu=\mu_{fT}\left(1+7.3\varphi+123\varphi^2\right), \tag{2.13}$$

where μ_0 is the reference viscosity. For water, $T_0=273K,\xi=-4.45$, and $\zeta=6.55$. In this paper, we choose $\mu_0$as the viscosity of the base fluid at the lower wall, so $\varsigma=-0.514$.

The thermal conductivity is predicted by the Maxwell-Garnett model [23]:

$$k=k_f\frac{k_s+2k_f-2\varphi\left(k_f-k_s\right)}{k_s+2k_f+\varphi\left(k_f-k_s\right)}\approx k_f(1-3\kappa\varphi), \tag{2.14}$$

$$\kappa=\frac{k_f-k_s}{2k_f+k_s}. \tag{2.15}$$

For alumina nanoparticles in water at room temperature, $k_f\sim1\mathrm{W}/(\mathrm{m}\cdot\mathrm{K}),k_s\sim40\mathrm{W}/(\mathrm{m}\cdot\mathrm{K})$[15], therefore, we assume $\kappa\sim-0.93$.

The above governing equations can be made dimensionless by the following transformations:

$$\begin{aligned}&\widetilde{\mathbf{u}}=\mathbf{u}/U_0,\widetilde{\rho}=\rho/\rho_f,\widetilde{\mu}=\mu/\mu_f,\widetilde{\varphi}=\varphi/\varphi_b,\\&\widetilde{T}=(T-T_b)\Big/\Delta T,\widetilde{\nabla}=\nabla\cdot d,\widetilde{t}=tU_0\Big/d.\end{aligned}\tag{2.16}$$

Here $U_0$is the reference velocity defined as follows:

$$U_0=\left(-\frac{\mathrm{d}p}{\mathrm{d}x}\right)d^2\Big/\left(8\mu_f\right),\tag{2.17}$$

d is the distance between two plane, $\varphi_b$is the average concentration, $T_b$is the temperature of the lower wall,$\Delta T=d\cdot\frac{\partial}{\partial x}T$is the temperature difference in the distance of d in x direction. Now the nanoparticle concentration is normalized:

$$\int_0^1\widetilde{\varphi}\mathrm{d}y=1.\tag{2.18}$$

The dimensionless governing equations are derived as follows:

$$\widetilde{\nabla}\cdot\widetilde{\mathbf{u}}=0,\tag{2.19}$$

$$\widetilde{\rho}Re\left(\frac{\partial\widetilde{\mathbf{u}}}{\partial\widetilde{t}}+\widetilde{\mathbf{u}}\cdot\widetilde{\nabla}\widetilde{\mathbf{u}}\right)=-\widetilde{\nabla}\widetilde{p}+\widetilde{\nabla}\cdot\left[\widetilde{\mu}\left(\widetilde{\nabla}\widetilde{\mathbf{u}}+(\widetilde{\nabla}\widetilde{\mathbf{u}})^{\mathrm{T}}\right)\right],\tag{2.20}$$

$$\frac{\partial\widetilde{T}}{\partial\widetilde{t}}+\widetilde{\mathbf{u}}\cdot\widetilde{\nabla}\widetilde{T}=\frac{1}{\mathrm{Re}\cdot Pr}\left[\widetilde{\nabla}\cdot\left(k\widetilde{\nabla}\widetilde{T}\right)+\frac{1}{Le}\left(\widetilde{D}_B\widetilde{\nabla}\widetilde{\varphi}+\widetilde{D}_T\frac{1}{N_{BT}}\widetilde{\nabla}\widetilde{T}\right)\cdot\widetilde{\nabla}\widetilde{T}\right],\tag{2.21}$$

$$\frac{\partial\widetilde{\varphi}}{\partial\widetilde{t}}+\widetilde{\mathbf{u}}\cdot\widetilde{\nabla}\widetilde{\varphi}=\frac{1}{Re\cdot Sc}\widetilde{\nabla}\cdot\left(\widetilde{D}_B\widetilde{\nabla}\widetilde{\varphi}+\widetilde{D}_T\frac{1}{N_{BT}}\widetilde{\nabla}\widetilde{T}\right).\tag{2.22}$$

Here the Reynolds number (Re), Prandtl number (Pr), Schmidt number (Sc) and Lewis number (Le) are defined as follows:

$$Re=\rho_fU_0d/\mu_f,\tag{2.23}$$

$$Pr=c\mu_f/k_f,\tag{2.24}$$

$$Sc=\frac{\mu_f}{\rho D_B^b},\quad D_B^b=\frac{k_BT_b}{3\pi\mu_fd_s},\tag{2.25}$$

$$Le=\frac{k}{(\rho c)_sD_B\varphi_b}.\tag{2.26}$$

The other parameters are defined as

$$\widetilde{D}_B=\frac{T}{\mu}\Big/\frac{T_b}{\mu_f},\quad\widetilde{D}_T=\frac{\varphi}{T}\Big/\frac{\varphi_b}{T_b},\tag{2.27}$$

$$N_{BT}=\frac{D_B^b\rho_fT_b}{\beta\mu_f\Delta T}.\tag{2.28}$$

The boundary conditions are set as follows:

$$\widetilde{\mathbf{u}}=0,\widetilde{D}_B\frac{\partial}{\partial y}\widetilde{\varphi}+\widetilde{D}_T\frac{1}{N_{BT}}\frac{\partial}{\partial y}\widetilde{T}=0,\quad y=0,1\tag{2.29a}$$

$$\widetilde{T}(0)=0,\widetilde{T}(1)=\Gamma.\tag{2.29b}$$

Here, $\Gamma$is the temperature difference of two walls in the normal direction.
We assume the flow is parallel, and its temperature is linear in x as imposed plus a distribution in y as follows:

$$\widetilde{\mathbf{u}}=(\widetilde{u}(y),0),\tag{2.30}$$

$$\widetilde{T}(x,y)=\pm x+\widetilde{T}_y(y),\tag{2.31}$$

where, $(+x)$stands for the convective cooling, while $(-x)$stands for the convective heating.

In (2.21), the temperature gradient has two components:$\widetilde{\nabla}\widetilde{T}=\frac{\partial\widetilde{T}}{\partial x}\mathbf{i}+\frac{\partial\widetilde{T}}{\partial y}\mathbf{j}$, where $\mathbf{i},\mathbf{j}$are the unit vectors in the x and y directions,

respectively. For simplicity, we assume that $1 = \left|\frac{\partial \widetilde{T}}{\partial x}\right| << \left|\frac{\partial \widetilde{T}}{\partial y}\right|$. This is also confirmed in the temperature distributions in Fig. 7 &10. Thus, we ignore the temperature gradient along the flow direction on the right side of (2.21). Similarly, we assume that the concentration of nanoparticles has $\widetilde{\varphi}(x,y) = \alpha x + \widetilde{\varphi}_y(y)$and $|\alpha| = \left|\frac{\partial \widetilde{\varphi}}{\partial x}\right| << \left|\frac{\partial \widetilde{\varphi}}{\partial y}\right|$.

Now the governing equations can be simplified as follows:

$$\frac{\mathrm{d}}{\mathrm{d}y}\left(\widetilde{\mu}\frac{\mathrm{d}}{\mathrm{d}y}\widetilde{u}\right) = -8, \tag{2.32}$$

$$\pm Pe\cdot\widetilde{u}(y) = \frac{\mathrm{d}}{\mathrm{d}y}\cdot\left(\widetilde{k}\frac{\mathrm{d}}{\mathrm{d}y}\widetilde{T}_y\right) + \frac{1}{Le}\left(\widetilde{D}_B\frac{\mathrm{d}}{\mathrm{d}y}\widetilde{\varphi} + \widetilde{D}_T\frac{1}{N_{BT}}\frac{\mathrm{d}}{\mathrm{d}y}\widetilde{T}_y\right)\cdot\frac{\mathrm{d}}{\mathrm{d}y}\widetilde{T}_y, \tag{2.33}$$

$$(Re\cdot Sc)\alpha\cdot\widetilde{u}(y) = \frac{\mathrm{d}}{\mathrm{d}x}\left(\widetilde{D}_B\alpha \pm \widetilde{D}_T\frac{1}{N_{BT}}\right) + \frac{\mathrm{d}}{\mathrm{d}y}\left(\widetilde{D}_B\frac{\mathrm{d}}{\mathrm{d}y}\widetilde{\varphi}_y + \widetilde{D}_T\frac{1}{N_{BT}}\frac{\mathrm{d}}{\mathrm{d}y}\widetilde{T}_y\right). \tag{2.34}$$

Here Pe is the Peclet number,

$$Pe = \mathrm{Re}\cdot Pr, \tag{2.35}$$

and two viscosity models and a thermal conductivity model have

$$\widetilde{\mu} = 1/(1-\varphi_b\widetilde{\varphi})^{2.5}, \tag{2.36}$$

$$\widetilde{\mu} = 1 + 7.3\varphi_b\widetilde{\varphi} + 123\varphi_b\widetilde{\varphi}^2, \tag{2.37}$$

$$k = 1 - 3\kappa\varphi_b\widetilde{\varphi}. \tag{2.38}$$

We suppose the parameters have the order as follows,

$$\mathrm{Re}\sim 40, Pr\sim 10, Pe\sim 400, \tag{2.39}$$

$$\varphi_b\sim 0.04, T_b\sim 350K, T_c\sim 320K, d\sim 0.01m, \Delta T = 0.2K. \tag{2.40}$$

Here, T_c is the temperature on the centre line $y = 0.5$.
The other parameters are estimated as follows [15],

$$Sc\sim 10^5, Le\sim 5\times 10^5, N_{BT}\sim 0.2\times 30 = 6,\ \ \kappa\sim -1. \tag{2.41}$$

As Le is very large, the right side of (2.33) is nearly independent of Le. So the effect of Lewis number on the result is not discussed in the following.

In (2.34), as $|\alpha| = \left|\frac{\partial \widetilde{\varphi}}{\partial x}\right| << \left|\frac{\partial \widetilde{\varphi}}{\partial y}\right|$, we have

$$\left|\frac{\mathrm{d}}{\mathrm{d}x}\left(\widetilde{D}_B\alpha\right)\right| << \left|\frac{\mathrm{d}}{\mathrm{d}y}\widetilde{D}_B\cdot\frac{\mathrm{d}}{\mathrm{d}y}\widetilde{\varphi}_y\right|, \left|\frac{\mathrm{d}}{\mathrm{d}x}\left(\widetilde{D}_T\frac{1}{N_{BT}}\right)\right| << \left|\frac{\mathrm{d}}{\mathrm{d}y}\left(\widetilde{D}_T\frac{1}{N_{BT}}\right)\cdot\frac{\mathrm{d}}{\mathrm{d}y}\widetilde{T}\right|, \tag{2.42}$$

the gradient along the flow direction on the right side of (2.34) can be neglected. Thus,

$$(Re\cdot Sc)\cdot\alpha\cdot\widetilde{u}(y) \approx \frac{\mathrm{d}}{\mathrm{d}y}\left(\widetilde{D}_B\frac{\mathrm{d}}{\mathrm{d}y}\widetilde{\varphi}_y + \widetilde{D}_T\frac{1}{N_{BT}}\frac{\mathrm{d}}{\mathrm{d}y}\widetilde{T}_y\right). \tag{2.43}$$

The integration along the vertical direction can be obtained with the boundary conditions in (2.29a),

$$(Re\cdot Sc)\cdot\alpha\cdot\int_0^1\widetilde{u}(y)\mathrm{d}y \approx \left(\widetilde{D}_B\frac{\mathrm{d}}{\mathrm{d}y}\widetilde{\varphi}_y + \widetilde{D}_T\frac{1}{N_{BT}}\frac{\mathrm{d}}{\mathrm{d}y}\widetilde{T}_y\right)\Big|_0^1 = 0. \tag{2.44}$$

As the mass flux $\int_0^1\widetilde{u}(y)\mathrm{d}y$ is the order of 1, $|\alpha| << 1$, and the left side of (2.34) can be neglected.

In this paper, we used the Chebyshev collocation method to solve the governing equations. N Chebyshev-collocation points$z = \left(1-\cos\left(\frac{j\pi}{N+1}\right)\right)\Big/2, j = 1\sim N$ are set in the flow region, while two points $z = 0, 1$ are set at the boundaries. The static flow is determined by the iteration method. We set the velocity field of plane Poiseuille flow of Newtonian fluid as the initial condition for the iteration, then T, $\varphi$and μ can be obtained, finally the velocity can be updated for the next iteration. And after several iterations, all the variables are convergent.

3. Numerical results

We consider ten cases with different parameters in Table 1, and four kinds of viscosity models in Table 2. Here, case (N) has $\varphi_b = 0$, which stands for the Newtonian fluid.

3.1. The case of convective cooling of laminar flows

First, we consider the case of convective cooling, where the temperature of the flow region is lower than that on the wall.

3.1.1. The distributions of nanoparticle concentration

The distributions of the nanoparticle concentration at $\Gamma = 0$ are displayed in Fig. 2. It can be seen that $\widetilde{\varphi}$ reaches its maximum at $y = 0.5$. The maximum of $\widetilde{\varphi}$ increases significantly with the increase of Pe (see curves (A), (D) in Fig. 2 (a)) and the decrease ofN_{BT} (see curves (A), (F) in Fig. 2 (a)). In Fig. 2 (b), we can find that the distributions of $\widetilde{\varphi}$ with model (II) are more concentrated in $y = 0.5$ than those with model (I). However, there is little variation for $\widetilde{\varphi}$when the effect of temperature on the viscosity is considered.

The distributions of $\widetilde{\varphi}$can be fitted by a Gaussian distribution after normalization,

Which can be seen in Fig. 3, and the standard deviation is shown in Table 3. When $\Gamma = 0$, it has

$$\widetilde{\varphi}(y) \approx \frac{1}{\sqrt{2\pi}\sigma} \cdot \exp\left(-\frac{(y-0.5)^2}{2\sigma^2} \right). \tag{3.1}$$

It can be seen in Table 3 that the standard deviation σ increases with the decrease of Pe and the increase of N_{BT}. However, κ and φ_b have little effect on σ. The value of σ can be obtained as follows. When the variations of μ, k, D_B along y axis are not too large, and $D_T \approx \varphi$, then (2.32)–(2.34) can be simplified as follows:

$$\frac{\mathrm{d}^2}{\mathrm{d}y^2} u \approx \frac{\mathrm{d}}{\mathrm{d}x} p = -8, \tag{3.2}$$

$$Pe \cdot u(y) \approx \frac{\mathrm{d}^2}{\mathrm{d}y^2} T_l, \tag{3.3}$$

$$\frac{\mathrm{d}^2}{\mathrm{d}y^2} \varphi + \frac{\mathrm{d}^2}{\mathrm{d}y^2} T \cdot \frac{1}{N_{BT}} \varphi \approx 0. \tag{3.4}$$

With the boundary conditions of u, we can deduce that

$$u \approx 4(1-y)y, \tag{3.5}$$

$$\frac{\mathrm{d}^2}{\mathrm{d}y^2} \varphi + 4(1-y)y \cdot \frac{Pe}{N_{BT}} \varphi \approx 0. \tag{3.6}$$

So comparing to the Gaussian distribution near the region $y = 0.5$, we have

$$\sigma \approx \sqrt{\frac{N_{BT}}{Pe}}. \tag{3.7}$$

However, when $N_{BT}$is small (Cases (H) & (I)), the thermophoresis makes more nanoparticles concentrate to the region with lower temperature. The stratifications of μ, k become more obvious. The approximations in (3.2)-(3.4) will lead to a large deviation and (3.7) is not valid.

Physically, the motion of nanoparticles can be seen as a superposition of the thermophoresis and Brownian diffusion [15]. Due to the former, nanoparticles concentrate to the centre of the flow region$y = 0.5$, which has the lowest temperature. In contrast, the

Table 1
10 kinds of parameters.

Case	κ	Pe	φ_b	N_{BT}
(A)	−0.93	400	0.02	9
(B)	−0.7	400	0.02	9
(C)	−0.93	200	0.02	9
(D)	−0.93	800	0.02	9
(E)	−0.93	400	0.04	9
(F)	−0.93	400	0.02	6
(G)	−0.93	400	0.02	20
(H)	−0.93	400	0.02	1
(I)	−0.93	400	0.02	0.3
(N)	−0.93	400	0.00	9

Table 2
4 kinds of viscosity models.

Case	μ
(I)	$\mu = \mu_f/(1-\varphi)^{2.5}$,
(II)	$\mu = \mu_f(1 + 7.3\varphi + 123\varphi^2)$,
(III)	$\mu = \mu_0 \exp\left(-0.51 - 4.45\left(\frac{T_0}{T}\right) + 6.55\left(\frac{T_0}{T}\right)^2\right)\Big/(1-\varphi)^{2.5}$,
(IV)	$\mu = \mu_0 \exp\left(-0.51 - 4.45\left(\frac{T_0}{T}\right) + 6.55\left(\frac{T_0}{T}\right)^2\right)(1 + 7.3\varphi + 123\varphi^2)$.

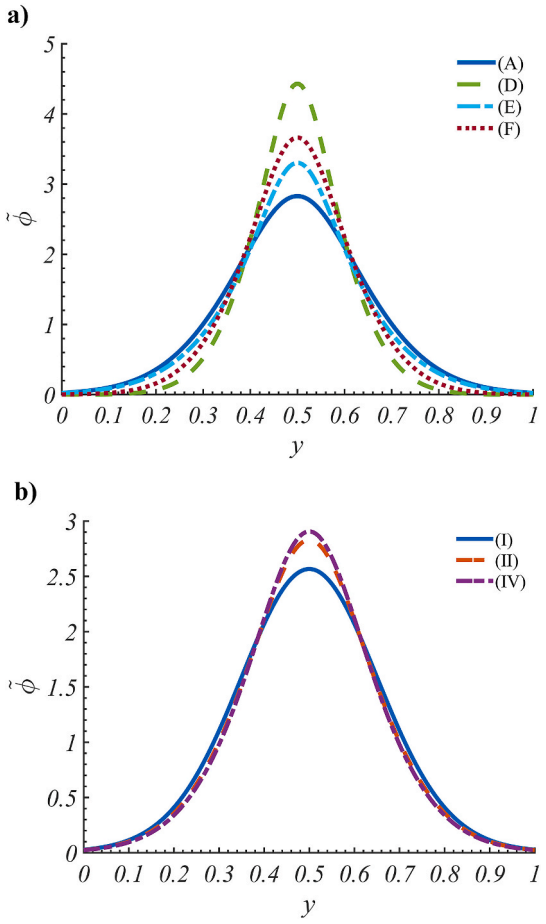

Fig. 2. The distributions of nanoparticle concentration at $\Gamma = 0$: (a) the results with viscosity model (II); (b) the comparisons of different viscosity models at case (A).

Brownian diffusion drives the nanoparticle away from the centre. Finally, these two effects reach an equilibrium. It is well known that the distribution of a free particle in the Brownian motion is Gaussian [24]. This can explain the reason for the distributions of $\widetilde{\varphi}$.

The Gaussian distribution can also be found when there is a temperature difference of between two walls, which is displayed in Fig. 3(b). By comparing with temperature distributions in Fig. 7(b), we find that the concentration reaches its maximum at the coldest region. The standard deviation increases with increase of Γ.

3.1.2. The distributions of viscosity

The distributions of the viscosity are displayed in Fig. 4. It can be seen that when $\Gamma = 0$,$\widetilde{\mu}$reaches its maximum at $y = 0.5$. The maximum of $\widetilde{\mu}$decreases with the increase of N_{BT}(see curves (A) and (F) in Fig. 4 (a)) and the decrease of Pe (see curves (A) and (C) in Fig. 4 (a)). Obviously, $\widetilde{\mu}$always increases with φ_b (see curves (A) and (E) in Fig. 4 (a)).

In Fig. 4 (b), we can find that the viscosities determined by four viscosity models differ from each other. The viscosity obtained by model (II) is larger than that by model (I). When the effect of temperature on the viscosity is considered, the viscosity stratification

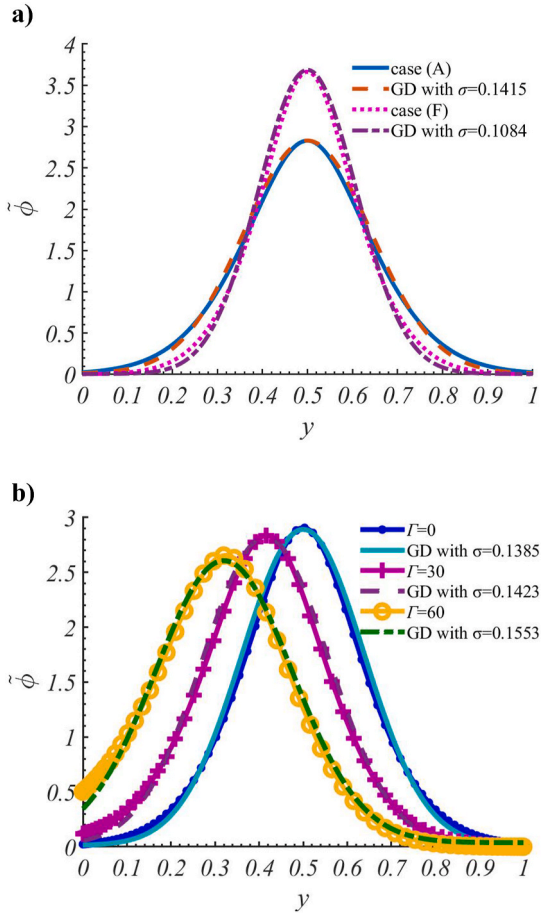

Fig. 3. Comparison of the distributions of $\tilde{\varphi}$ and Gaussian distributions: (a) the results with viscosity model (II) at $\Gamma = 0$; (b) the results with viscosity model (IV) at differentΓ. Here, GD stands for Gaussian distribution.

Table 3
The standard deviations of Gaussian distributions with viscosity model (II).

Standard deviation	(A)	(B)	(C)	(D)	(E)	(F)
σ	0.1415	0.1410	0.2100	0.0899	0.1202	0.1084

becomes lager.

As $\varphi_b$is small, we have

$$\mu = 1 \Big/ (1 - \varphi_b\varphi)^{2.5} \approx 1 + 2.5\varphi_b\varphi, \tag{3.8}$$

for the viscosity model (I) and

$$\mu \approx 1 + 7.3\varphi_b\varphi, \tag{3.9}$$

for the viscosity model (II). So μ and $\tilde{\mu}$ also have Gaussian distributions. When $|y - 0.5| > 0.2$, $\tilde{\mu}$ tends to 1 as $\varphi \to 0$.

When $\Gamma > 0$, the increase of $\tilde{\mu}$ at $y = 0$is caused by the increase of nanoparticle concentration, while the decrease of $\tilde{\mu}$ at $y = 1$is caused by the increase of temperature. The maximum of $\tilde{\mu}$ decreases by the increase of Γ.

We can see that there are obvious stratifications for the viscosity in Fig. 4, which can be caused by both the nanoparticle concentration and the temperature effect. In Fig. 6, the effect of viscosity stratifications on the velocity distribution is not very obvious. However, previous works have found that the viscosity stratifications have a great impact on the flow instability [25,26]. This suggests that the instability of nanofluid flows maybe very different from that of Newtonian fluid flows.

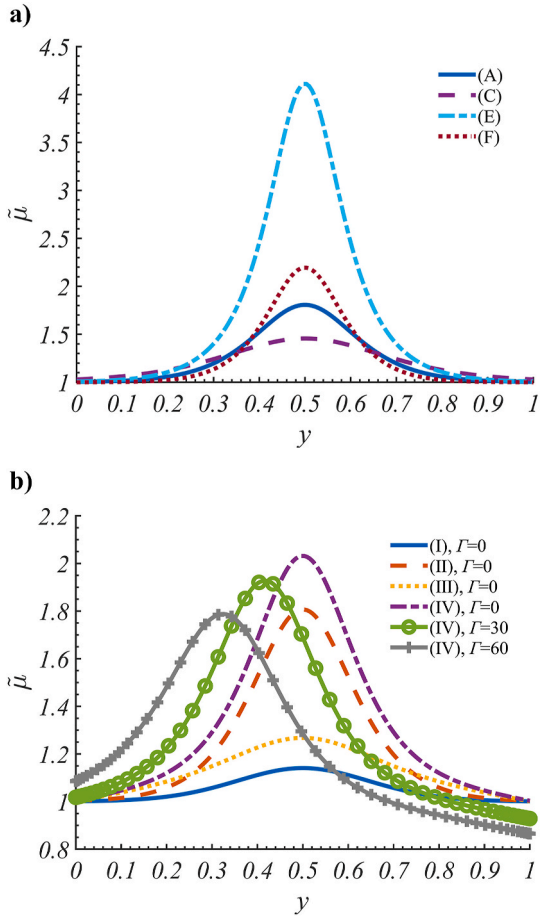

Fig. 4. The distributions of viscosity: (a) the results with viscosity model (II) at $\Gamma = 0$; (b) the comparisons of different viscosity models at case (A).

3.1.3. *The distributions of thermal conductivity*

The distributions of the thermal conductivity are displayed in Fig. 5. The results with viscosity model (II) are shown in Fig. 5. It can be seen that $\widetilde{k}$ reaches its maximum at $y = 0.5$. The maximum of $\widetilde{k}$ increases with the increase of Pe (see curves (A) and (D) in Fig. 5) and the decrease of N_{BT} (see curves (A) and (F) in Fig. 5).

Obviously, $\widetilde{k}$always increases with φ_b (see curves (A) and (E) in Fig. 5). When κ becomes smaller (see curves (A) and (B) in Fig. 5), the stratification of $\widetilde{k}$decreases. As k has a linear relationship with φ in (2.38), the thermal conductivity also has a Gaussian distribution

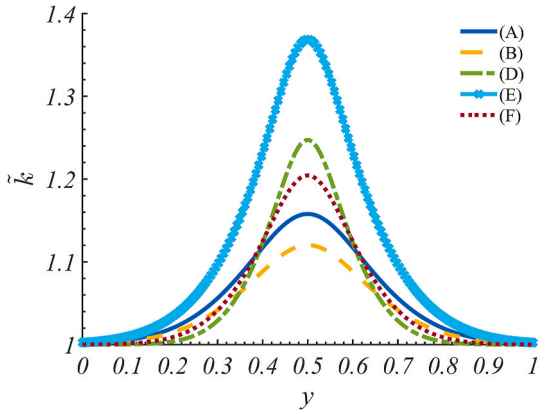

Fig. 5. The distributions of thermal conductivity with viscosity model (II) at $\Gamma = 0$.

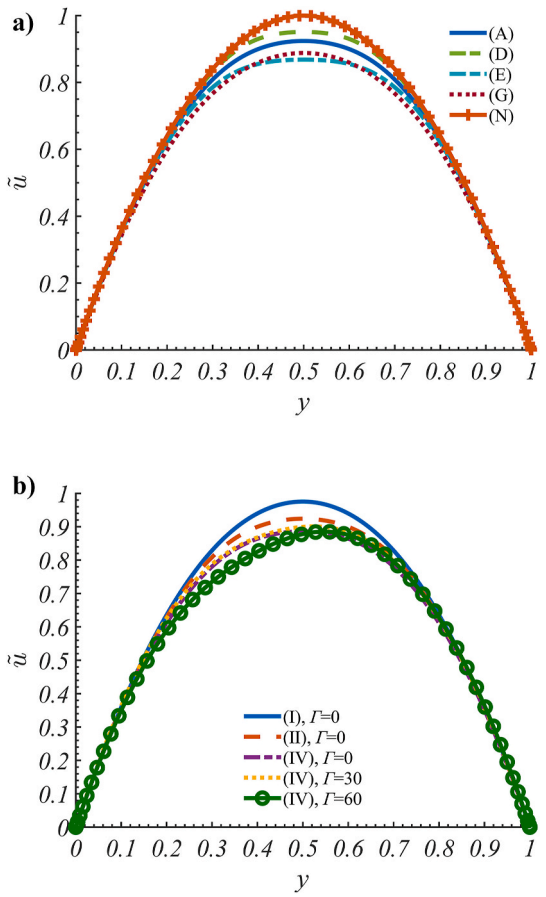

Fig. 6. The distributions of velocity: (a) the results with viscosity model (II) at $\Gamma = 0$; (b) the comparisons of different viscosity models and Γat case (A).

after normalization. The thermal conductivity is not sensitive to the viscosity model.

3.1.4. *The distributions of velocity*

The distributions of the velocity are displayed in Fig. 6. Comparing with the case of Newtonian fluid (see curve (N) in Fig. 6 (a)), there is only a little decrease for the velocity in the cold region.$\widetilde{u}$reaches its maximum at $y = 0.5$. The maximum of $\widetilde{u}$increases with the increase of *Pe* (see curves (A) and (D) in Fig. 6 (a)) and the decrease of φ_b (see curves (A) and (E) in Fig. 6 (a)). However, N_{BT}has little effect on the velocity (see curves (A) and (G) in Fig. 6 (a)). Fig. 6 (b) shows that there is a slight decrease for the velocity when the temperature effect on the viscosity is considered. The effect of $\Gamma$for the velocity is not obvious.

3.1.5. *The distributions of temperature*

The distributions of the temperature are displayed in Fig. 7. It can be seen that $\widetilde{T}$reaches its minimum at $y = 0.5$. With the decrease of *Pe*, the minimum of $\widetilde{T}$increases significantly (see curves (A) and (C) in Fig. 7 (a)). WhenN_{BT}decreases, the minimum of $\widetilde{T}$ decreases slightly (see curves (A) and (F) in Fig. 7 (a)). The minimum of $\widetilde{T}$increases with the increase of φ_b(see curves (A) and (E) in Fig. 7 (a))and Γ(see Fig. 7 (b)). Meanwhile, the temperature distribution is not sensitive to the viscosity model.

3.2. *The case of convective heating of laminar flows*

Then we pay attention to the case of convective heating, where the temperature of the flow region is higher than that on the wall.

3.2.1. *The distributions of nanoparticle concentration*

The distributions of the nanoparticle concentration are displayed in Fig. 8, where the viscosity model (II) is used. In contrast to the case of convective cooling, when $\Gamma = 0$,$\widetilde{\varphi}$ reaches its minimum at $y = 0.5$, while its maximum is reached at the wall. The minimum of $\widetilde{\varphi}$is obviously larger than zero, which differs from the case of convective cooling (see Fig. 2).The minimum of $\widetilde{\varphi}$ decreases significantly with the increase of *Pe* (see curves (A) (C) in Fig. 8), and the decrease ofN_{BT} (see curves (A), (G) in Fig. 8). However, the variation of

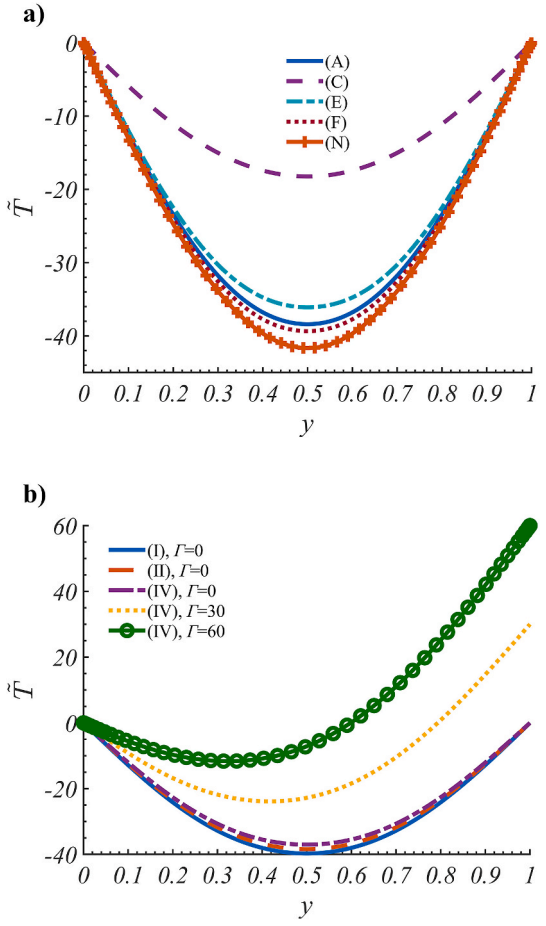

Fig. 7. The distributions of temperature: (a) the results with viscosity model (II) at $\Gamma = 0$; (b) the comparisons of different viscosity models and Γat case (A).

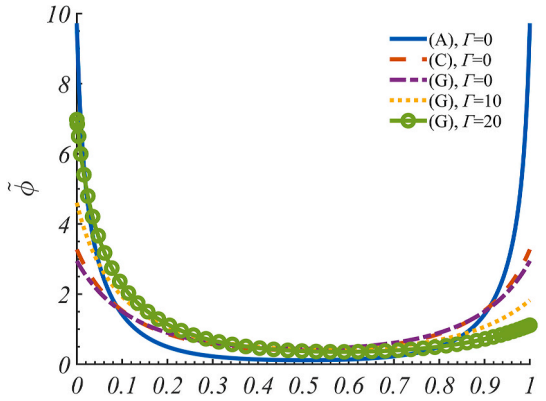

Fig. 8. The distributions of nanoparticle concentration with viscosity model (II).

φ_b(see curves (A) (E) in Fig. 8), and κ have little effect on $\widetilde{\varphi}$. When Γincreases, the maximum of $\widetilde{\varphi}$appears at the cold wall, where the value of $\widetilde{\varphi}$ increases with Γobviously.

3.2.2. The distributions of thermal conductivity and viscosity

The distributions of the thermal conductivity and viscosity are displayed in Fig. 9, where the viscosity model (II) is used. Due to the nanoparticle concentration, the distributions of the thermal conductivity and viscosity of convective heating are opposite to the case of

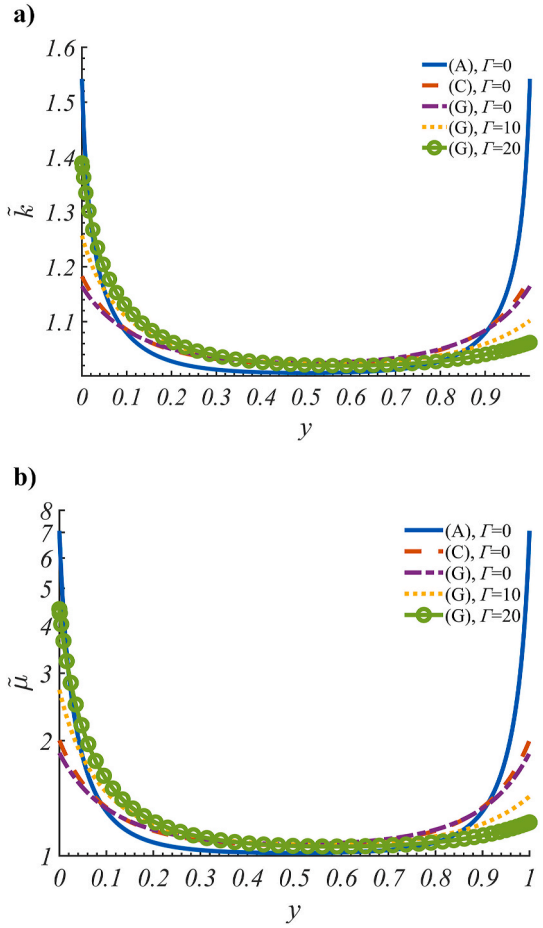

Fig. 9. The distributions of (a) thermal conductivity and (b)viscosity with model (II).

convective cooling (see Figs. 4 and 5).

3.2.3. The distributions of velocity and temperature

The distributions of the velocity and temperature are displayed in Fig. 10. When $\Gamma = 0$, $\tilde{u}$reaches its maximum at $y = 0.5$. The maximums of$\tilde{u}, \tilde{T}$decrease significantly with the increase of φ_b(see curves (N), (A) in Fig. 10). The effects of Γ, Pe and N_{BT}on the velocity are not obvious.

Compared to the case of convective cooling (see Figs. 6 and 7), the decreases of the amplitudes of $\tilde{u}, \tilde{T}$at the case of convective heating are much larger. This can be explained as follows. The temperature distribution highly depends on the velocity distribution, which is closely related to the viscosity. For the convective heating, when $\Gamma = 0$,$\tilde{\varphi}$ reaches its maximum at the wall, where the shear stress is large. Due to the nanoparticle concentration near the wall, the viscosity increases, and the shear rate decreases significantly. In contrast, when $\Gamma = 0$,$\tilde{\varphi} \approx 0$near the wall for the convective cooling. Therefore, the increase of nanoparticle has less effect on the velocity.

4. Conclusion

In this work, the plane Poiseuille flow of nanofluids in the channel with linearly varying wall temperature is investigated numerically. The cases of convective cooling and heating of laminar flows are considered, respectively. The distributions of the nanoparticle concentration, thermal conductivity, viscosity, velocity and temperature are determined.

For convective cooling, the temperature on the wall is higher than that in the flow region in the normal direction. Due to the temperature difference and thermophoresis force, nanoparticles move from hot region to the cold one. Thus, the nanoparticles concentration φ has a Gaussian distribution in the normal direction, and reaches its maximum at the coldest region. When the temperature difference of two walls $\Gamma = 0$, the standard deviation has $\sigma \approx \sqrt{N_{BT}/Pe}$, where N_{BT} stands for the ratio of Brownian diffusivity to thermophoretic diffusivity. The distribution of nanoparticles by viscosity model (II) is more concentrative than that by viscosity model (I).

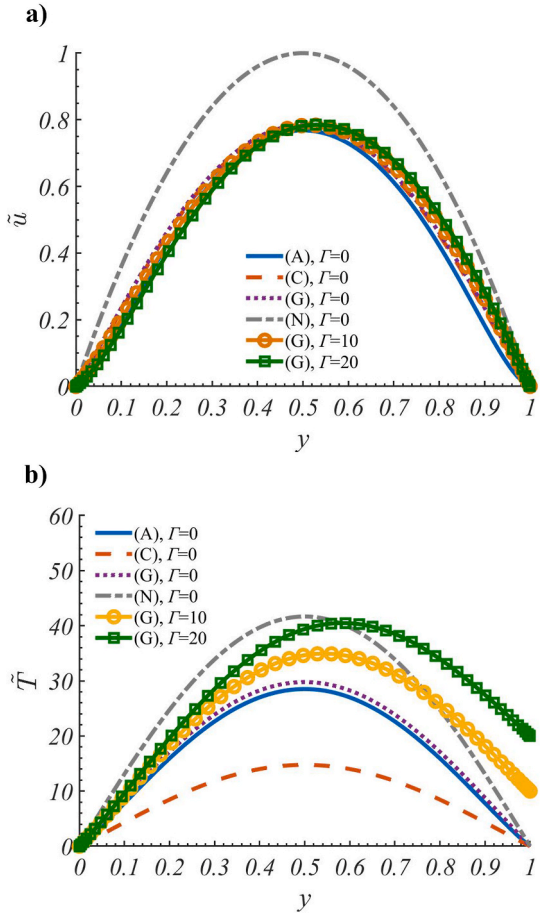

Fig. 10. The distributions of (a) velocity and (b) temperature.

Due to the linear relationship of thermal conductivity k and φ, the thermal conductivity also has a Gaussian distribution after normalization. The viscosity μ increases with the increase of Pe and the decrease of N_{BT}. When the average volume fraction of nanoparticle is small, there is a linear relation between $\varphi$and μ, thus μ also has a Gaussian distribution after normalization.

Comparing with the case of Newtonian fluid, there is only a little decrease for the velocity in the cold region. The amplitudes of velocity and temperature increase with the increase of Pe and are nearly independent on N_{BT}. The increase of nanoparticle concentration leads to a little decrease for the velocity. When the temperature dependent viscosity model is used, the viscosity stratification becomes lager, while the variations of velocity and temperature are small.

For convective heating, the distributions of the nanoparticle concentration, thermal conductivity and viscosity are opposite to those at convective cooling. φ reaches its minimum at the hottest region, which is obviously larger than zero. As φ reaches its maximum at the wall, the velocity and temperature decrease significantly.

Declaration of competing interest

We declare that we have no financial and personal relationships with other people or organizations that can inappropriately influence our work, there is no professional or other personal interest of any nature or kind in any product, service and company that could be construed as influencing the position presented in, or the review of, the manuscript entitled, “The nanofluid flows in the channel with linearly varying wall temperature”.

Acknowledgments

This work has been supported by the National Natural Science Foundation of China (Nos.11872032 and 11772344), Zhejiang Provincial Natural Science Foundation (LY21A020006), K. C. Wong Magna Fund and the Special research funding from the Marine Biotechnology and Marine Engineering Discipline Group in Ningbo University(No.422004582).

References

[1] S.U.S. Choi, D.A. Singer, H.P. Wang, Developments and applications of non-Newtonian flows, ASME FED 66 (1995) 99–105.
[2] S. Kakaç, A. Pramuanjaroenkij, Review of convective heat transfer enhancement with nanofluids, Int. J. Heat Mass Tran. 52 (13–14) (2009) 3187–3196.
[3] Y. Xuan, Q, Li, Eat transfer enhancement of nanofluids, Int. J. Heat Fluid Flow 21 (1) (2000) 58–64.
[4] D. Wen, G. Lin, S. Vafaei, K. Zhang, Review of nanofluids for heat transfer applications, Particuology 7 (2) (2009) 141–150.
[5] J. Philip, P.D. Shima, Thermal properties of nanofluids, Adv. Colloid Interface Sci. 183 (2012) 30–45.
[6] S.A. Angayarkanni, J. Philip, Review on thermal properties of nanofluids: recent developments, Adv. Colloid Interface Sci. 225 (2015) 146–176.
[7] M. Sheikholeslami, H.B. Rokni, Magnetic nanofluid flow and convective heat transfer in a porous cavity considering Brownian motion effects, Phys. Fluids 30 (1) (2018), 012003.
[8] M. Hojjat, S.Gh Etemad, R. Bagheri, J. Thibault, Rheological characteristics of non-Newtonian nanofluids: experimental investigation, Int. Commun. Heat Mass Tran. 38 (2) (2011) 144–148.
[9] J. Kang, F. Zhou, W. Tan, T. Xia, Thermal instability of a nonhomogeneous power-law nanofluid in a porous layer with horizontal throughflow, J. Non Newton, Fluid Mech. 213 (2014) 50–56.
[10] M.A. Sheremet, I. Pop, M.M. Rahman, Three-dimensional natural convection in a porous enclosure filled with a nanofluid using Buongiorno's mathematical model, Int. J. Heat Mass Tran. 82 (2015) 396–405.
[11] R. Jusoh, R. Nazar, I. Pop, Three-dimensional flow of a nanofluid over a permeable stretching/shrinking surface with velocity slip: a revised model, Phys. Fluids 30 (3) (2018), 033604.
[12] Y. Jiang, X. Zhou, Analysis of flow and heat transfer characteristics of nanofluids surface tension driven convection in a rectangular cavity, Int. J. Mech. Sci. 153 (2019) 154–163.
[13] S.M. Vanaki, P. Ganesan, H.A. Mohammed, Numerical study of convective heat transfer of nanofluids: a review, Renew. Sustain. Energy Rev. 54 (2016) 1212–1239.
[14] X. Si, H. Li, L. Zheng, Y. Shen, X. Zhang, A mixed convection flow and heat transfer of pseudo-plastic power law nanofluids past a stretching vertical plate, Int. J. Heat Mass Tran. 105 (2017) 350–358.
[15] J. Buongiorno, Convective transport in nanofluids, J. Heat Tran. 128 (3) (2006) 240–250.
[16] F. Garoosi, F. Talebi, Numerical analysis of conjugate natural and mixed convection heat transfer of nanofluids in a square cavity using the two-phase method, Adv. Powder Technol. 28 (7) (2017) 1668–1695.
[17] S. Ostrach, Combined Natural and Forced Convection Laminar Flow and Heat Transfer of Fluids with and without Heat Sources in Channels with Linearly Varying Wall Temperatures, NACA Technical Note, 1954.
[18] R.K. Shahand, A.L. London, Laminar Flow Forced Convection in Ducts: a Source Book for Compact Heat Exchanger Analytical Data, Academic press, 2014.
[19] H.C. Brinkman, The viscosity of concentrated suspensions and solutions, J. Chem. Phys. 20 (4) (1952), 571-571.
[20] S.E.B. Maiga, S.J. Palm, C.T. Nguyen, G. Roy, N. Galanis, Heat transfer enhancement by using nanofluids in forced convection flows, Int. J. Heat Fluid Flow 26 (4) (2005) 530–546.
[21] F. Garoosi, M.M. Rashidi, Conjugate-mixed convection heat transfer in a two-sided lid-driven cavity filled with nanofluid using Manninen's two phase model, Int. J. Mech. Sci. 131 (2017) 1026–1048.
[22] B.C. Pak, Y.I. Cho, Hydrodynamic and heat transfer study of dispersed fluids with submicron metallic oxide particles, Exp. Heat Tran. 11 (2) (1998) 151–170.
[23] M. Narayana, P. Sibanda, Laminar flow of a nanoliquid film over an unsteady stretching sheet, Int. J. Heat Mass Tran. 55 (25–26) (2012) 7552–7560.
[24] I. Karatzas, S. Shreve, Brownian Motion and Stochastic Calculus, Springer Science & Business Media, 2012.
[25] C. Nouar, I. Frigaard, Stability of plane Couette–Poiseuille flow of shear-thinning fluid, Phys. Fluids 21 (6) (2009), 064104.
[26] R. Govindarajan, K.C. Sahu, Instabilities in viscosity-stratified flow, Annu. Rev. Fluid Mech. 46 (2014) 331–353.

Nomenclature

$\Psi, \widetilde{\Psi}$: Ψ is a variable, $\widetilde{\Psi}$ is its dimensionless form
c: nanofluid specific heat $(\mathrm{J}/(\mathrm{kg}\cdot\mathrm{K}))$
d: the distance between two plane (m)
d_s: nanoparticle diameter (m)
D_B: Brownian diffusion coefficient (m^2/s)
D_B^b: Brownian diffusion coefficient under the wall temperatureT_b (m^2/s)
D_T: thermal diffusion coefficient (m^2/s)
k: nanofluid thermal conductivity $(\mathrm{W}/(\mathrm{m}\cdot\mathrm{K}))$
k_B: Boltzmann constant (J/K)
k_f: base fluid thermal conductivity$(\mathrm{W}/(\mathrm{m}\cdot\mathrm{K}))$
k_s: nanoparticle thermal conductivity$(\mathrm{W}/(\mathrm{m}\cdot\mathrm{K}))$
Le: Lewis number
N_{BT}: ratio of Brownian and thermophoretic diffusivities
p: pressure (Pa)
Pe: Peclet number
Pr: Prandtl number
Re: Reynolds number
Sc: Schmidt number
t: time (s)
T: nanofluid temperature (K)
T_0: reference temperature (K)
T_b: the temperature of the lower wall (K)
$\boldsymbol{u}$: nanofluid velocity (m/s)
U_0: reference velocity (m/s)

Greek

α: the concentration gradient along the flow direction
β: thermophoretic coefficient
Γ: the temperature difference of two walls in the normal direction
$\boldsymbol{\tau}$: stress tensor (Pa)
ρ: nanofluid density (kg/m^3)
μ: viscosity $(\mathrm{Pa}\cdot\mathrm{s})$
μ_0: reference viscosity $(\mathrm{Pa}\cdot\mathrm{s})$

μ_f: base fluid viscosity $(\mathrm{Pa}\cdot\mathrm{s})$
μ_{fT}: base fluid viscosity under the influence of temperature$(\mathrm{Pa}\cdot\mathrm{s})$
φ: nanoparticle concentration
φ_b: average concentration
ρ_s: nanoparticle density $(\mathrm{kg/m^3})$
ρ_f: base fluid density $(\mathrm{kg/m^3})$
κ: ratio of thermal conductivities between base fluid and nanoparticle
ΔT: temperature difference in the distance of d in x direction (K)